Chapter 4

I-V Mismatch in PV Generators

The current-voltage (I-V) characteristic of a PV generator is obviously the result of all the I-V curves of the elements which it is made of. For a PV panel's characteristic the single series-connected solar cells have to be considered, for a string all the series-connected PV modules, while for a complex array all the strings parallel-connected. Unfortunately, the I-V characteristic of an element differs nearly from that of the other ones, arising the problem known as "mismatching". The causes can be various, like the manufacturing tolerance, i.e., the pattern of crystalline domains in poly-silicon cells, or the different ageing or temperature of each element of the PV generator, or in the presence of not uniformly distributed shade over the PV array. These phenomena can cause important losses in the energy production of the generator, but they could also lead to destructive effects, such as "hot spots", or even the breakdown of single solar cells.
The aim of this chapter is to expose the mismatch in a PV generator, with a particular focus on that from partial shading. First of all, the induced modification in the solar cell parameters is investigated, through experimental measurements and simulations on a single PV module. Then a real BIPV system case study is presented and it is used as a laboratory for analysing the consequence of the current-voltage mismatch on the elements of a PV system in terms of power losses. The case study presented is exploited through all this dissertation for presenting experimental studies on a mismatched PV array and its grid-connected inverter.

4.1 Series/parallel mismatch in the I-V characteristic

Firstly, it will be worthy to explain the I-V mismatch in general for the solar cells, making a classification in series and parallel mismatch. In the first case the effect of the different short-circuit current (and maximum power point current) of each solar cell is that the total I-V characteristic of a string of series-connected cells can be constructed summing the voltage of each cell at the same current value, fixed by the worst element of the string. This means that the string I-V curve is strongly limited by the short-circuit current of the bad cell, and consequently the total output power is much less than the sum of each cell maximum power.
This phenomenon is more relevant in the case of shading than in presence of production tolerance. A bad cell does not perform as an open circuit, but like a low resistance (a few ohms or a few tens of ohms), becoming a load for the other solar cells. In particular, it is subject to an reverse voltage and it dissipates power, then if the power dissipation is too high, it will be possible the formation of some "hot spots", with degradation and early ageing of the solar cell. Furthermore, if the reverse voltage applied to a shaded cell exceeds its breakdown value, it could be destroyed.
The worst situation is with the string in short-circuit, when all the voltage of the irradiated cells is applied to the shaded ones. It is clear that the most dangerous case occurs if the shaded cell is only one, while the experience shows that usually with two shaded cells the heating is still acceptable.
The solution adopted worldwide for this problem is the by-pass diode in anti-parallel connection with a group of solar cells, typically one or two (in parallel) diodes for each group of twenty cells. In this way, the output power decreases only of the contribution of the group of bad cells and the reverse voltage is limited by the diode.
In the case of parallel of strings, it is the voltage mismatch which becomes important. The total I-V characteristic can be constructed summing the current of each string at the same voltage value. The total open-circuit voltage will be very close to that of the bad string.
The worst case for the bad or shaded string is that one of the open circuit, be-

cause it will become the only load for the other strings. Consequently, it will conduct inverse current with unavoidable over-heating, which can put the string out of service. In the parallel mismatching a "blocking" diode in series with the string can avoid the presence of inverse currents.
In the next section the study of the series mismatch is presented for the real case of a PV module subject to partial shading, in which the influence of this phenomenon on the solar cell model parameters is investigated.

4.2 I-V mismatch on PV panel because of partial shading

In order to study a real case of partial shading, with irregularly-shaped shade affecting also part of the solar cells' area, at first the I-V characteristic distortion induced by modification of solar cell model parameters and the by-pass diode switched on is investigated.
The same PV panel analysed in the previous chapter is considered and the same experimental analysis is performed on it, firstly, with one single solar cell shaded, then with half solar cell shaded, parallel to its metal ribbons, so with half solar cell affected by a shade perpendicular to its metal ribbons, and finally with two halves of two different solar cells shaded and two by-pass diodes switched on.
In order to simulate the I-V characteristic with some cells shaded, a fist set of parameters is computed assuming the solar irradiance and cell temperature equal to those of the totally irradiated PV module and considering all the experimental data measured. The results are parameters which allow to simulate the irradiated solar cells of the module.
Secondly, only the samples of the experimental I-V characteristic relative to the "shaded zone" are considered, where the by-pass diode does not operate since the panel current value is equal or less than that of the shaded cell. In this way, it is possible to compute the I_{ph} for the shaded cell and indirectly have information about the solar irradiance over its surface.
Also the other solar cell model parameters are evaluated in these experimental conditions, in order to be able to simulate with good accuracy the I-V curve of

the shaded cell.

The next step is to reconstruct the I-V characteristics of the twenty cell block, in irradiated and shaded conditions from the two sets of parameters computed and the characteristic of the by-pass diode. This because the by-pass diodes are in parallel with block of twenty cells and, if one or more of them are shaded, all the cells of the same block are shunted by the diode. Fig. 4.1 shows the two I-V curves reconstructed. Finally the I-V curve of the whole PV module with

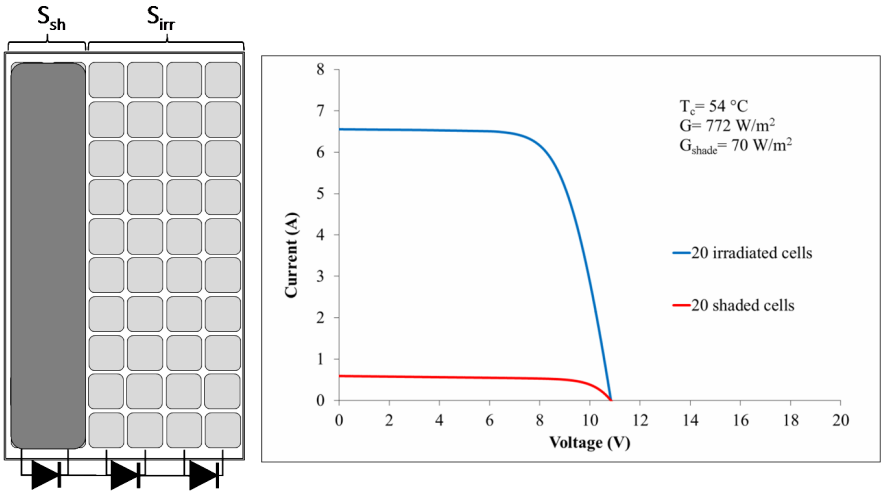

Figure 4.1: I-V curves of 20 solar cell blocks in irradiated and shaded conditions.

1 shaded cell is built combining properly the single block characteristics, that is summing the voltage of two irradiated blocks and one shaded block for each value of cell string current. The result is illustrated in Fig. 4.2, in which the RMSD for the I-V curve is equal to 0.060 A. When the two cases with shade over half solar cell are considered, as expected the solar irradiation over the shaded cell rises and so does accordingly the photo-generated current. Figures 4.4 and 4.6 show the simulation results for these two cases, and the RMSDs for the modelled I-V curves are 0.077 A and 0.083 A.

The last case, illustrated in Fig. 4.8, is that of two shaded halves of solar cell, with the intervention of two different by-pass diodes since the resulting solar irradiation over the two shaded zones differs slightly, causing a small mismatch also between the two 20 cell blocks with the shaded half cell. Therefore, the

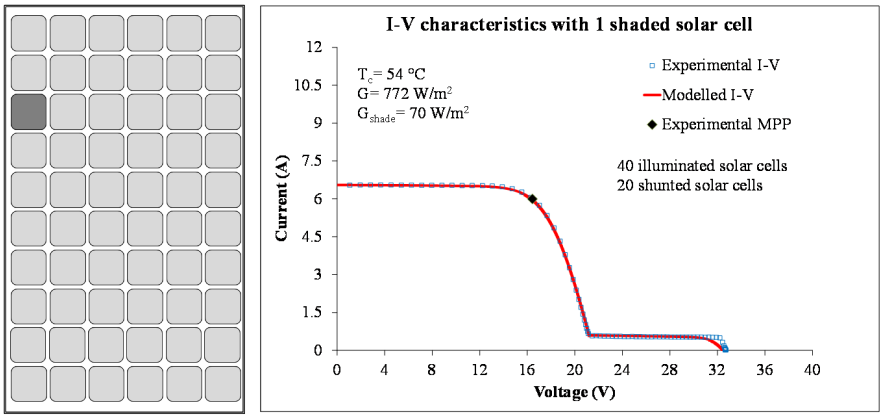

Figure 4.2: I-V and P-V curves of a PV module with 1 shaded cell (model and experimental).

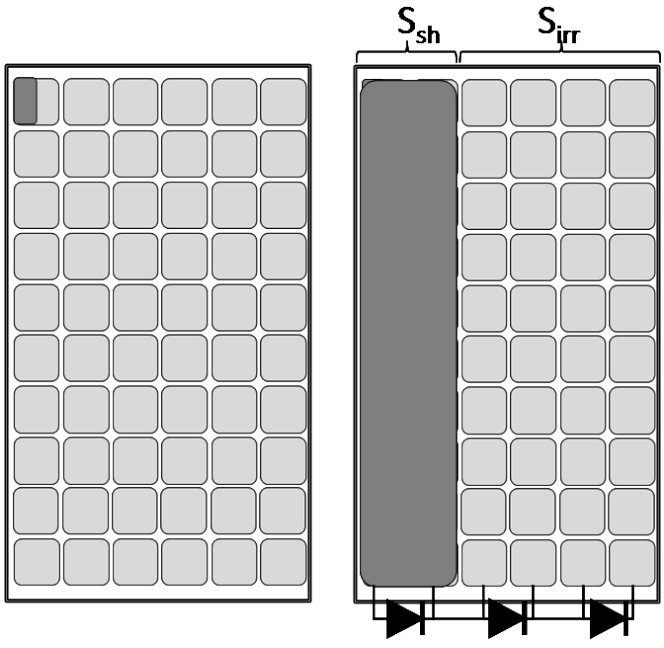

Figure 4.3: Equivalence between half shaded cell (case 1) and 20 shaded cells due to by-pass diode.

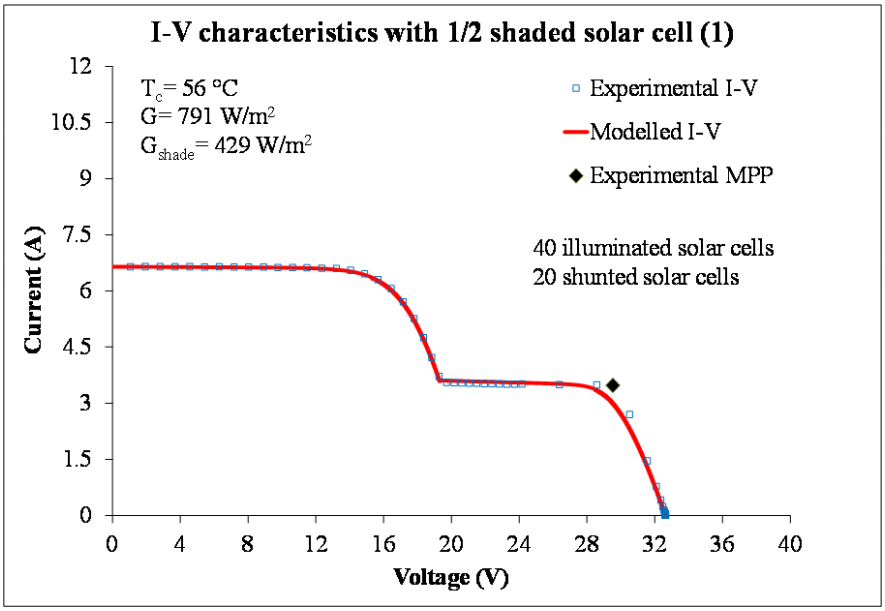

Figure 4.4: I-V and P-V curves of a PV module with 1/2 shaded cell, case 1 (model and experimental).

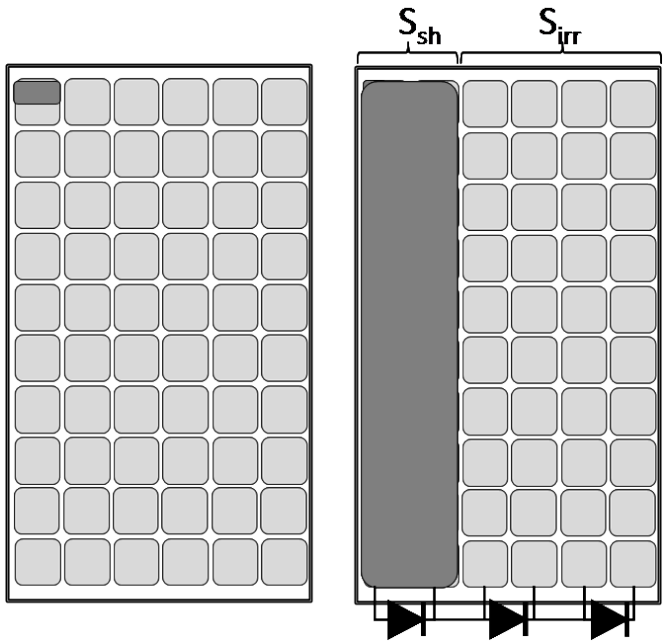

Figure 4.5: Equivalence between half shaded cell (case 2)and 20 shaded cells due to by-pass diode.

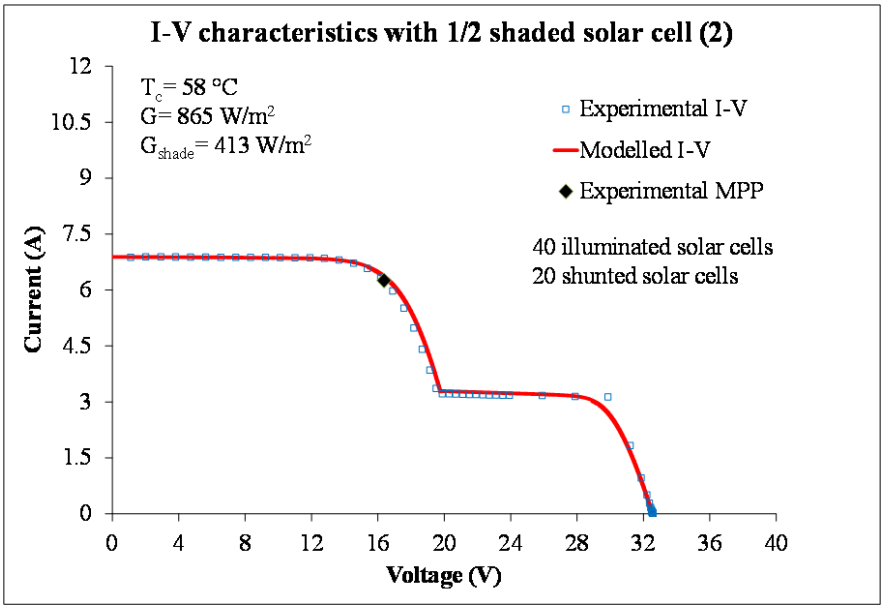

Figure 4.6: I-V and P-V curves of a PV module with 1/2 shaded cell, case 2 (model and experimental).

simulation in this case has requested the evaluation also of the photo-generated current in the first shaded zone, that labelled with 1 in the picture, while the other cell parameters are supposed equal to those resulting for the shaded zone 2. The RMSD in this case is of 0.152 A.

It is needed to be stressed that the greatest simulation error is performed in the zone of the I-V characteristic near the V_{OC}, where the current generated by the shaded cells drops abruptly. This error is not avoidable, because for following the real behaviour, rectangular-shaped, the model should imply a I_0 almost null, which is not conceivable. The Table 4.1 resumes all the parameter sets computed in order to obtain the simulated curves in Figures 4.2–4.8.

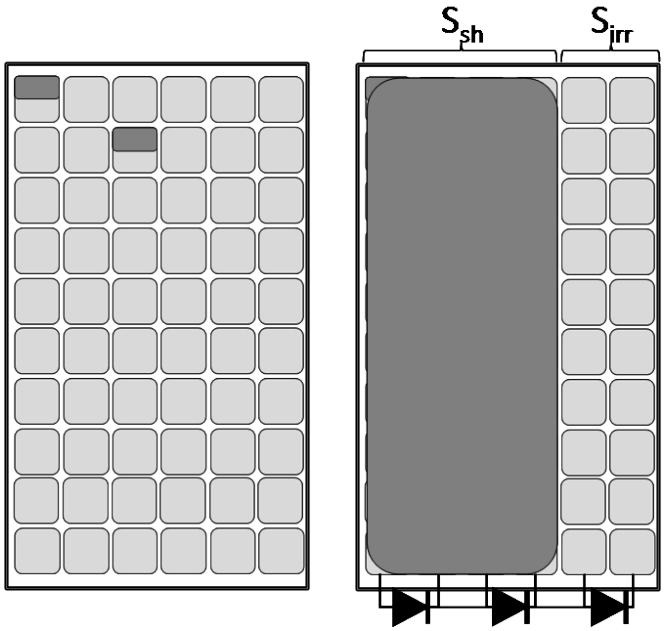

Figure 4.7: Equivalence between 2 half shaded cells and 40 shaded cells due to 2 by-pass diodes.

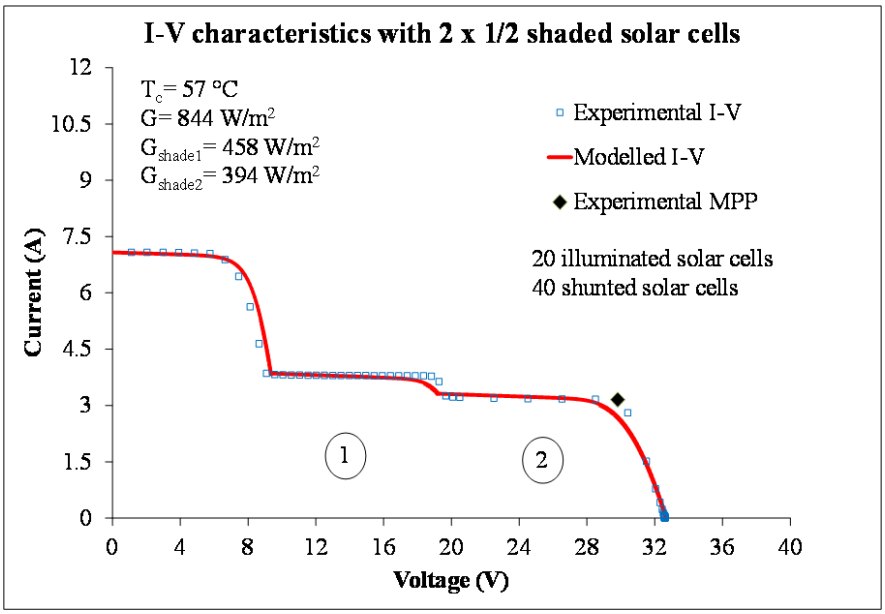

Figure 4.8: I-V and P-V curves of a PV module with two 1/2 shaded cells (model and experimental).

Solar Cell Parameters in Experimental Conditions

Shaded Cells	**Area**	I_{ph}**(A)**	I_0**(A)**	m**(p.u.)**	$R_{sh}(\Omega)$	R_s**(m**Ω**)**	V_{OC}**(V)**	I_{SC}**(A)**	V_{mpp}**(V)**	I_{mpp}**(A)**	MPP**(W)**	G**(W/m^2)**	T_c**(°C)**
1	S_{irr}	6.56	1.5 x 10$^-$7	1.10	9.35	8	0.54	6.55	0.27	6.02	1.65	772	54
	S_{sh}	0.59	1.9 x 10$^-$9	1.0	6.98	13	0.54	0.59	0.53	0.53	0.28	70	54
1/2 case 1	S_{irr}	6.65	1.7 x 10$^-$7	1.10	11.06	8	0.54	6.65	0.49	3.48	1.71	791	56
	S_{sh}	3.61	1.5 x 10$^-$8	1.0	3.98	4	0.54	3.60	0.49	3.48	1.71	429	56
1/2 case 2	S_{irr}	6.89	2.1 x 10$^-$7	1.10	14.68	7	0.54	6.89	0.27	6.25	1.71	865	58
	S_{sh}	3.29	1.6 x 10$^-$8	1.0	3.43	3	0.54	3.29	0.50	3.14	1.56	413	58
2 x 1/2	S_{irr}	7.10	2.0 x 10$^-$7	1.10	3.65	8	0.54	7.09	0.50	3.15	1.57	844	57
	S_{sh1}	3.85	1.5 x 10$^-$8	1.0	3.09	3	0.54	3.85	0.32	3.77	1.20	458	57
	S_{sh2}	3.32	1.5 x 10$^-$8	1.0	3.09	3	0.54	3.31	0.50	3.15	1.57	394	57

Table 4.1: Solar Cell Parameters in Experimental Conditions.

It can be noted that the value of R_{sh} decreases in the zones where the by-pass diode does not intervene, since the slope of the almost-constant current tract of the I-V is greater than at higher level of current. Correctly, the importance of the parallel leakage current is higher when the photo-generated current is lower. Also the value of the R_s usually decreases, in order to follow the steep drop of the current near the V_{OC}, but this is less clear from a physical point of views, since it could depend on the temperature rise of the shaded cell, but the measurements are performed with the PV module at open circuit condition and without giving the time necessary to the cell temperature to change when solar cell are shaded, so the mentioned temperature should not change. This is confirmed by the simulated I-V curves of the shaded cells, which are not translated respect the position given by the cell temperature of the irradiated cells. The Table 4.2 presents the solar cell parameters at STC relative to the MPP and open-circuit and short-circuit conditions. It is evident the Fill Factor drop due to the partial shading effect, also with shade only on part of a solar cell.

Solar Cell Parameters in STC

No. shaded cells	V_{OC} **(V)**	I_{SC} **(A)**	V_{mpp} **(V)**	I_{mpp} **(A)**	P_{mpp} **(W)**	FF **(p.u.)**
0	0.60	8.35	0.47	7.64	3.59	0.71
1	0.60	8.34	0.30	7.66	2.31	0.46
1/2 case 1	0.60	8.25	0.54	4.32	2.34	0.47
1/2 case 2	0.60	7.80	0.30	7.09	2.15	0.46
2 x 1/2	0.60	8.24	0.55	3.67	2.02	0.41

Table 4.2: Solar Cell Parameters in STC.

4.3 BIPV specific non-idealities: Case Study

In this section the Building Integrated PV system considered as a Case Study is described. This system is the subject of all the analysis performed about the influence of I-V mismatch in PV array and inverter performance of BIPV plants, as well as the Power Quality studies which will constitute the last part of this

dissertation. A general description follows, pointing out all the particularities which affect it, together with the main technical data.

4.3.1 Large Commercial BIPV system

The real BIPV system considered is characterized by a 834.5 kW_p rated power and it is installed on the top of an industrial building, a clothing wholesale warehouse, in the outskirts of Turin (Italy), partly for self-consumption, partly for power injection in the grid. The whole PV generator is composed of two different sub-fields of 778.61 kW_p and 55.89 kW_p, with mono-crystalline and poly-crystalline silicon modules, respectively (Fig. 4.9). All the PV arrays are connected on the LV side through 8 three-phase inverters, 6 for the first section, with different power ratings, and 2 for the second one. The inverters and the LV/MV transformer are oversized for minimizing losses and maximizing lifespan. The total rated powers are 873 kVA for the inverters and 1250 kVA for the Δ/Y transformer. The PV arrays have been installed with the aim of maximizing the occupation of the roof surface on the commercial building, accepting the occurrence of partial shading during the day on some arrays. The first field is South-West oriented, consequently the exposition to the solar radiation is neither symmetrical nor optimal and is different during morning and evening. The second field is optimally (South) oriented and not integrated (less thermal losses), being fix-mounted on a flat side terraces. Fig. 4.10 shows the geometrical layout of the PV arrays. Two PV arrays (no. 4 and 5) are subject to systematic partial shading. These arrays have the same rated power (98 kW_p) and their inverters have rated powers of 100 kVA each. The shading patterns projected by various obstacles, such as the borders of the triangular-shape shed, differ in the two parts of the day. The array no. 5 is subject to partial shading during the morning (Fig. 4.11). The same effect appears on the adjacent array no. 4 during the afternoon, when the array no. 5 is not shaded any longer. Even if the architectonic obstructions are not negligible in this case study, the majority of the arrays in the PV system are not subject to shading. In fact, the arrays no. 1, 2, 3, 6, 7 and 8, accounting for a total of 638 kW_p, are always exposed to the direct beams in spring and summer during the central sunlight hours (as an example, Fig. 4.12 shows the I-V and

P-V curves measured during the operation of the array no. 1, indicating that no shading occurs). In the structure non-linear loads made by fluorescent lamps are present, since the illumination is guaranteed from 8:00 a.m. to 8:00 p.m.. The loads include machines for air conditioning, personal computers and a data processing centre. These loads are not balanced over the three supply phases and this has great effects on the overall unbalance of the current three-phase system, as it will be illustrated in the chapter 6.

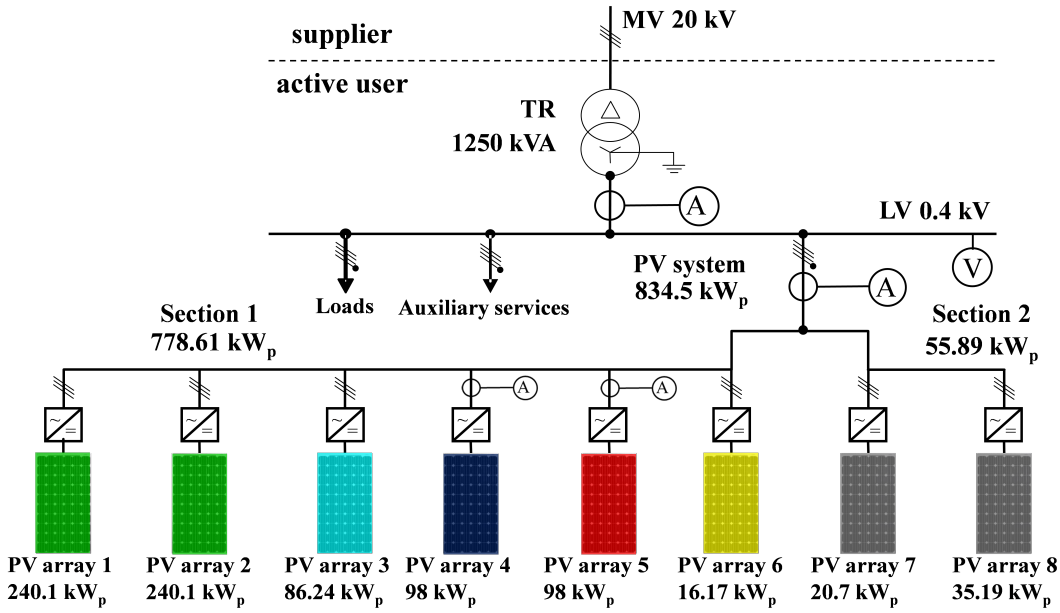

Figure 4.9: Electrical scheme of the PV system under study.

4.3.2 Technical specifications

The technical data, such as the electrical and mechanical specifications, of the main PV system components under study (PV module with m-Si cells, array no. 5 and its inverter) are reported in Tables 4.3–4.5 .

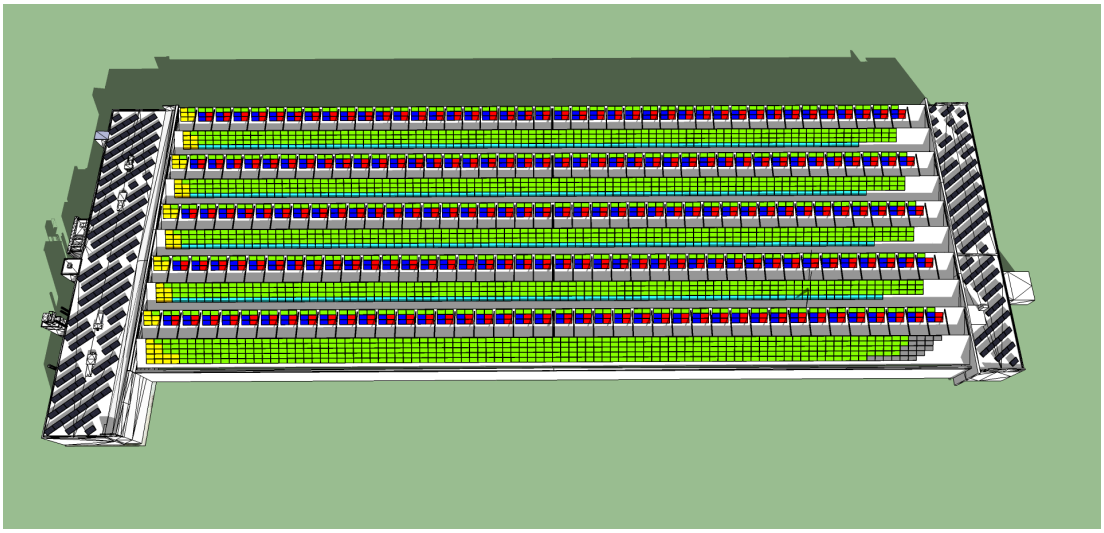

Figure 4.10: Geometrical layout of the PV system under study. The colours of the arrays match with the ones indicated in Fig. 4.9.

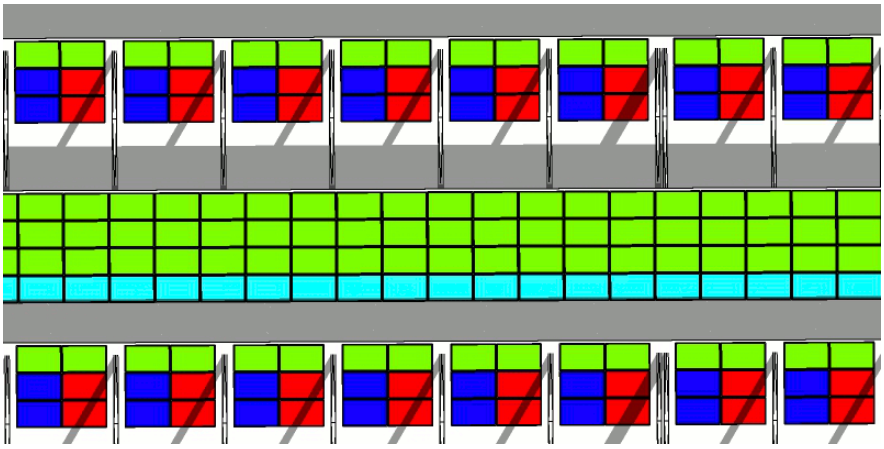

Figure 4.11: Particular of the partial shading over the 98 kW_p PV array no. 5 (red panels) at hour 12:15 a.m. in January.

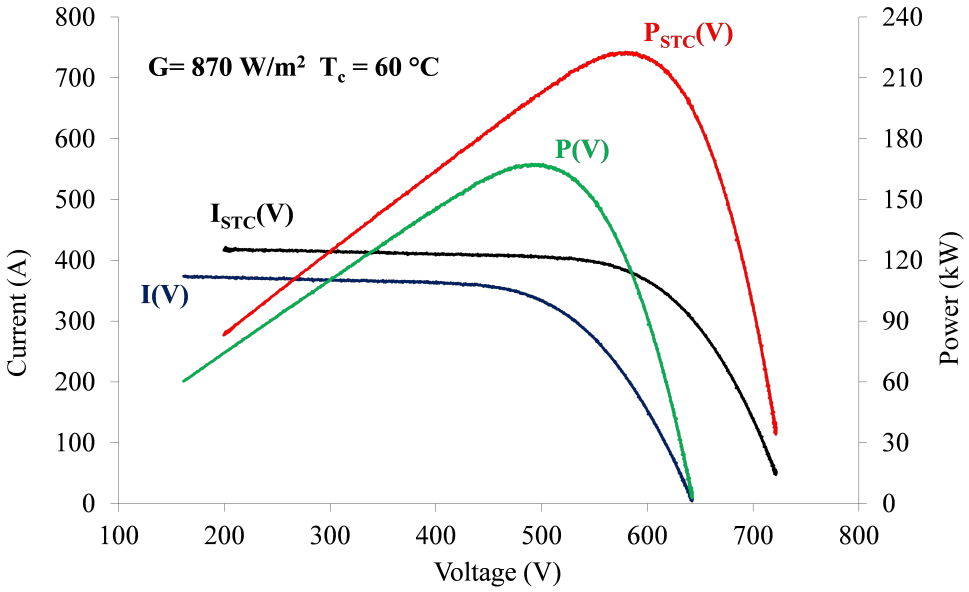

Figure 4.12: Experimental results (I-V and P-V curves), on PV array no. 1 with 240 kW_p in a Spring day. Actual data and values reported to the Standard Test Conditions (STC).

Parameter	**Value**	
$\mathbf{P_{rated}}$	245	W
$\mathbf{V_{mpp}}$	30.3	V
$\mathbf{I_{mpp}}$	8.09	A
$\mathbf{V_{OC}}$	37.4	V
$\mathbf{I_{SC}}$	8.61	A
$\eta_{\mathbf{PV}}$	15.23	%
$\mathbf{T_{operation}}$	$-40 \div 85$	℃
$\gamma_{\mathbf{T}}$	-0.45	%/K
$\alpha_{\mathbf{T}}$	$+0.06$	%/K
$\beta_{\mathbf{T}}$	-0.35	%/K
Cell type	m-Si (15.6 x 15.6)	cm
Cell no.	60	
Dimensions	1638 x 982 x 40	mm

Table 4.3: PV module's datasheet.

Parameter	**Value**	
No.modules/string	20	
No.strings	20	
$\mathbf{P_n}$	98.0	kW_p
$\mathbf{V_{mpp}}$	606.0	V
$\mathbf{I_{mpp}}$	161.8	A
$\mathbf{V_{OC}}$	748.0	V
$\mathbf{I_{SC}}$	172.2	A

Table 4.4: Array no.5 electrical parameters.

Parameter	Value	
$\mathbf{P_n}$	100.0	kVA
$\eta_{\mathbf{max}}$	97.1	%
$\eta_{\mathbf{european}}$	96.5	%

Table 4.5: Inverter no.5 specifics.

4.4 I-V mismatch effect on PV array

Once the impact of a partial shading on a single module has been clarified, even when a small part of a single solar cell is shaded, the more complex case of an array in a real BIPV system can be considered. A measurement campaign has been carried out on the BIPV system presented in the section 4.3, and in particular on the array no. 5, in order to study the current-voltage characteristic modifications and overall performance losses of the whole system, constituted by array and its inverter, due to the shading. The measurements on the PV array no. 5 have been repeated at different hours, in the morning, following the evolution of the shade, shown in Fig. 4.13 for a pair of PV modules of the array, which repeats itself the same for each of the 200 pairs of panels which the PV array is made by. It can been noted that the shade due to the tie-beams is limited to few cells, partially or completely covered. This is sufficient to cause the intervention of one or more by-pass diodes for each panel. For each measurement the I-V curve has been acquired with the capacitor method at open circuit, as exposed in the chapter 3, electrically separating the PV array from its inverter, then, re-connecting the PV array, the voltages and currents have been measured at DC and AC side of the inverter. With the sufficient stability of the environment conditions, this procedure allows to match the static P-V characteristic of the PV array, together with its absolute maximum power point (P_{MPP}), with the MPP tracker (MPPT) working point of the inverter. Furthermore, the inverter efficiency is computed at the corresponding DC input power (or P_{AC}/P_n as well). Fig. 4.14 illustrates the measurement scheme adopted for the data acquisition, while Fig.s 4.15, 4.16, 4.17, 4.18 and 4.19 show the resulting I-V curves (in red), P-V curves (in green), MPPT working point (in blue) and the point of the P_{MPP} (black triangles).

Following the curves' evolution it can be appreciated with how much efficiency the MPPT follows the absolute maximum points on the P-V curves of the array (Fig. 4.20).

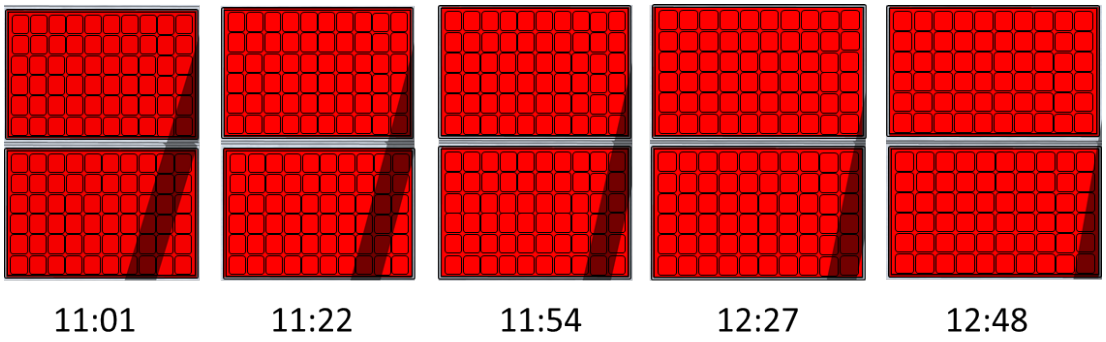

Figure 4.13: Time evolution of the shading over the array no. 5 in the late morning of a day in July 2012 (the hours are indicated under the corresponding pair of PV modules)

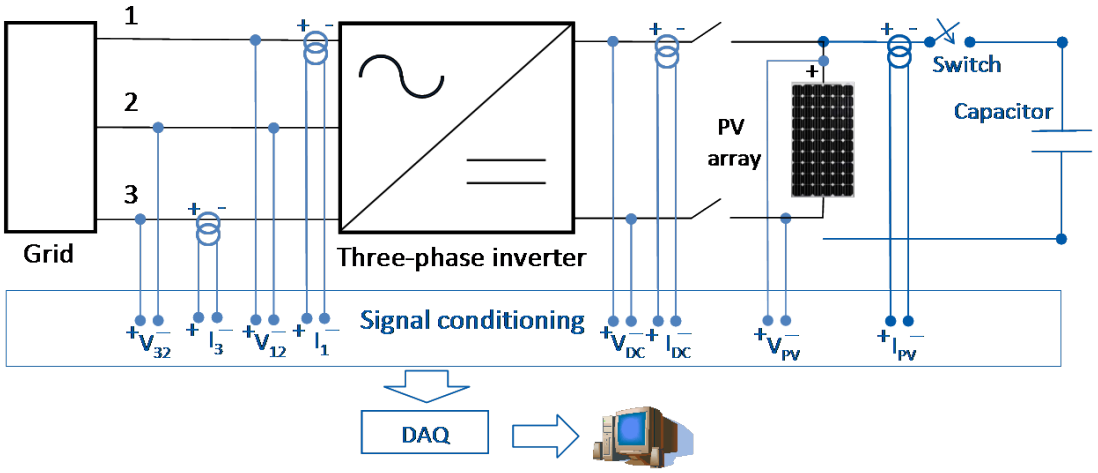

Figure 4.14: Measurement scheme for signal acquisition on PV array no. 5 and its inverter.

In Table 4.6 it can be observed that, for the PV array n.5, the power losses for the curve deformation go from 66% to 30% with respect to the theoretical value P_{lim} which takes into consideration only the influence of solar irradiance

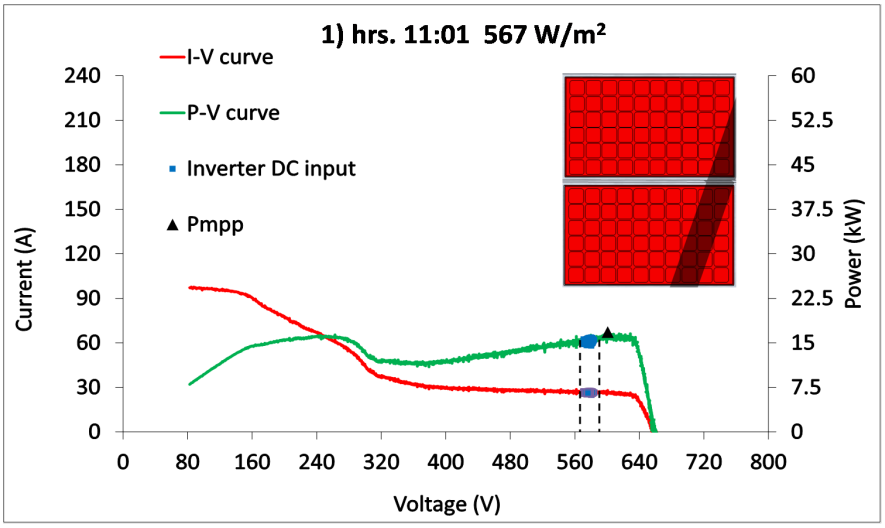

Figure 4.15: I-V and P-V curve of array no. 5 at 11:01 in a day of July 2012.

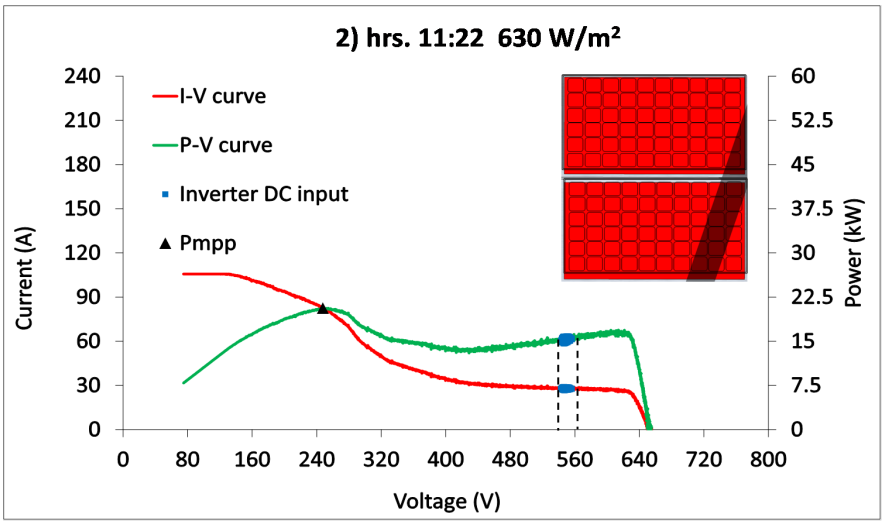

Figure 4.16: I-V and P-V curve of array no. 5 at 11:22 in a day of July 2012.

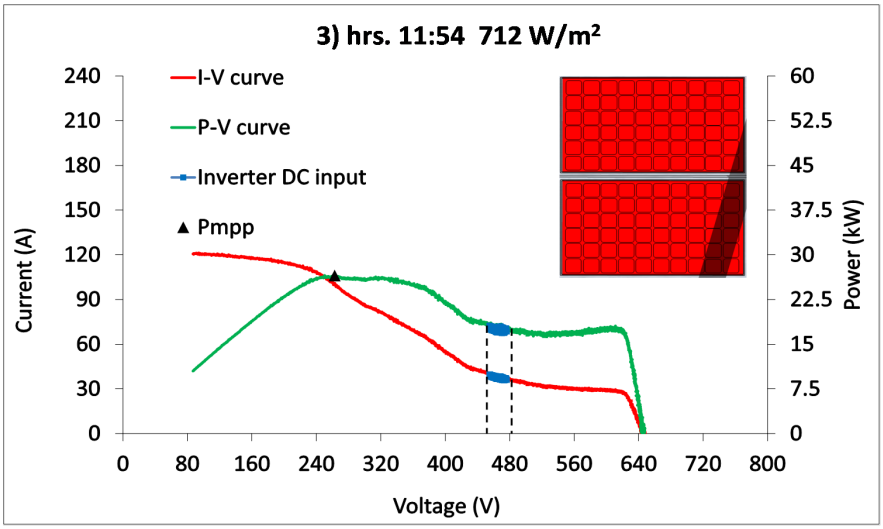

Figure 4.17: I-V and P-V curve of array no. 5 at 11:54 in a day of July 2012.

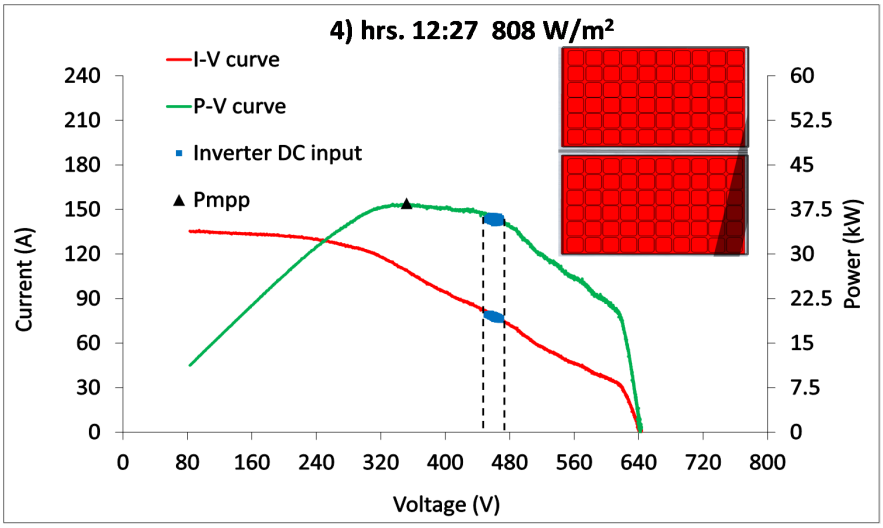

Figure 4.18: I-V and P-V curve of array no. 5 at 12:27 in a day of July 2012.

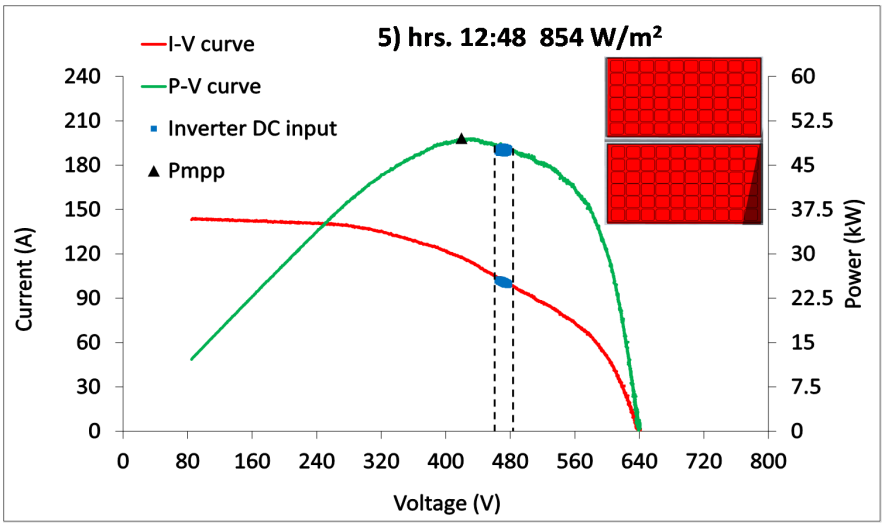

Figure 4.19: I-V and P-V curve of array no. 5 at 12:48 in a day of July 2012.

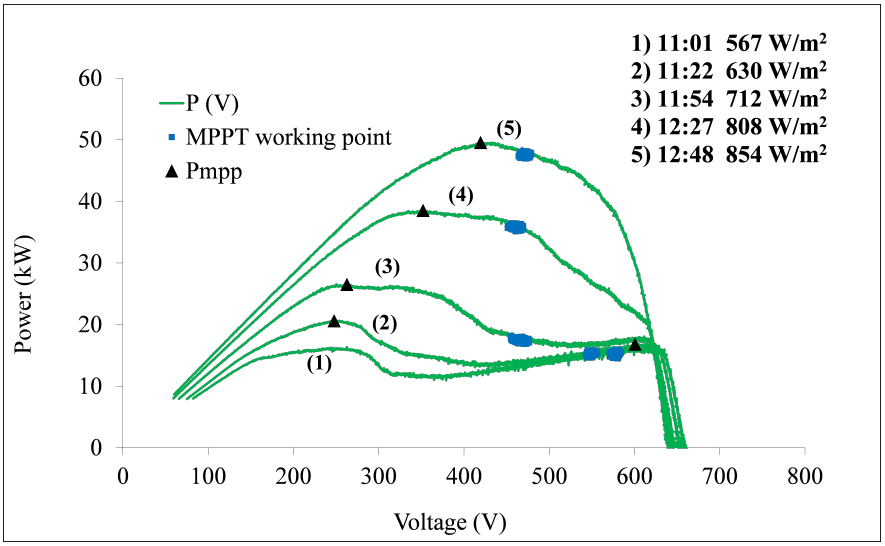

Figure 4.20: Time evolution of the P-V curves of the array no. 5 in the late morning of a day in July 2012.

and estimated cell temperature, so given by

$$P_{lim} = P_{rated}\frac{G}{1000}\left(1 + \gamma\Delta T_c\right) \tag{4.1}$$

and

$$\Delta P_{MPP} = \frac{P_{MPP} - P_{lim}}{P_{lim}} \times 100 \tag{4.2}$$

Obviously, there is not linearity between irradiated surface and the value of P_{MPP} as it is illustrated in Fig. 4.21

	Shaded cells per panel pair	S_{irr} **(%)**	P_{MPP} **(kW)**	P_{lim} **(kW)**	ΔP_{MPP} **(%)**	G **(W/m^2)**	T_c **(°C)**
1	17	85.83	16.8	49.5	66	567	49
2	15	87.50	20.6	54.3	62	630	52
3	11	90.83	26.5	60.5	56	712	55
4	7	94.17	38.5	67.3	43	808	58
5	4	96.67	49.6	70.5	30	854	60

Table 4.6: P_{MPP}, P_{lim} and ΔP_{MPP} at some experimental conditions (G, T_c) and percentage of totally irradiated surface S_{irr}.

4.5 I-V mismatch effect on inverter

The last main element of the BIPV system whose performance is affected by the I-V mismatch is the inverter. Let's continue to analyse the case of array no. 5 of the case study of this dissertation. The inverter performance can be assessed both on DC side and AC side. On DC side the attention has been pointed to the following parameters:

- the ripple peak factors of DC voltage V_{pp} and current I_{pp}, defined as:

$$V_{pp} = \frac{V_{max} - V_{min}}{V_{avg}} \tag{4.3}$$

$$I_{pp} = \frac{I_{max} - I_{min}}{I_{avg}} \tag{4.4}$$

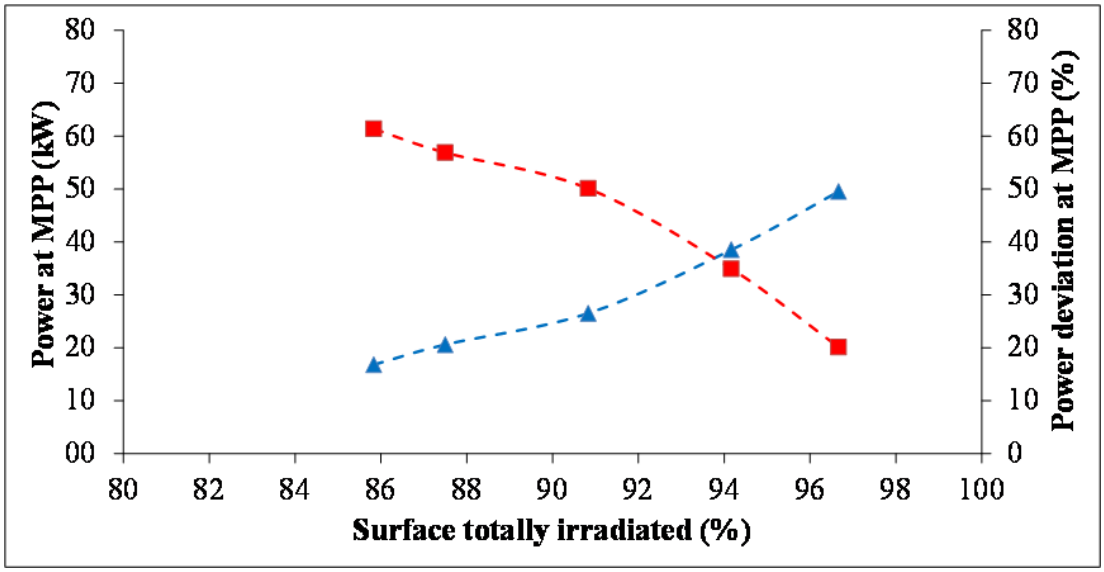

Figure 4.21: P_{MPP} and ΔP_{MPP} vs. totally irradiated surface.

where V_{max}, V_{min} and V_{avg} are the maximum, minimum and average value of the instantaneous voltage in the observation window (the current parameters have the same meanings);

- the MPP Tracker efficiency (how close to P_{MPP} the MPPT is operating):

$$\eta_{MPPT} = \frac{P_{DC}}{P_{MPP}} \tag{4.5}$$

where P_{DC} is the input power of the inverter.

In the case of the five measurements done during the partial shading of array no. 5, with each of the five I-V curves an acquisition of the DC voltage and current has been performed during a 0.2 seconds time window, like that in Fig. 4.22 Therefore the ripple peak factors and MPPT efficiencies have been computed for all the available measurements, as reported in Table 4.7 and in Fig. 4.23. The results show that the MPPT efficiency is very low at low input DC power, when the I-V curve is very deformed and there are more than one local maximum, while it increases if the input power grows. It can be stated that the MPPT algorithm seems to be switched off at low power levels, remaining anchored near

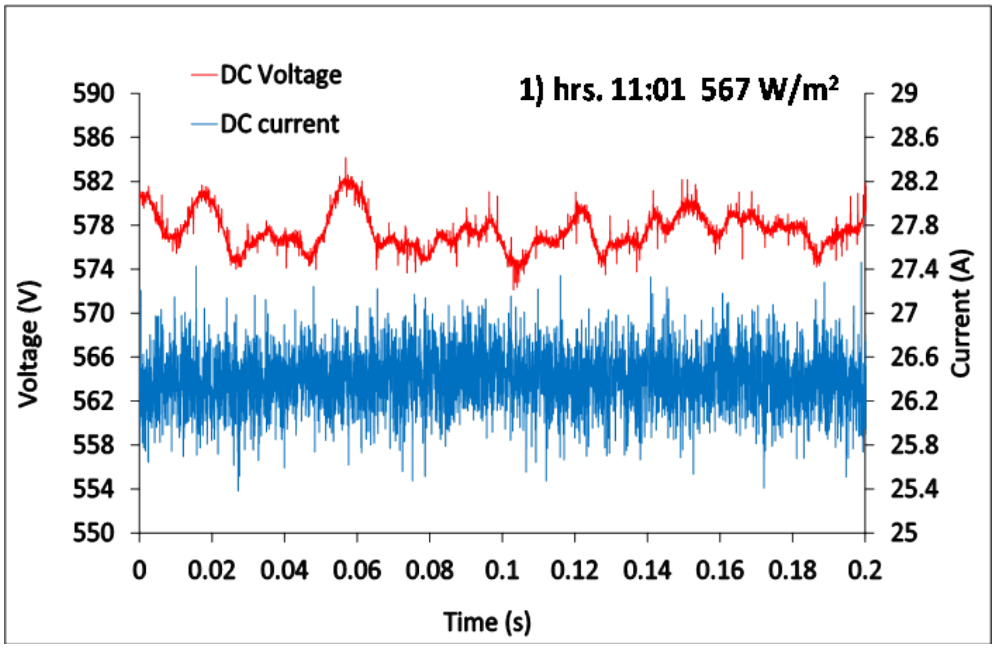

Figure 4.22: DC voltage and current at the inverter no. 5 input.

a certain voltage value, while restarts to follow the absolute maximum when the input power is sufficient to make it recognizable.

	V_{pp}	I_{pp}	P_{DC} (kW)	P_{MPP} (kW)	η_{MPPT}
1	2.3%	9.3%	15.2	16.8	90.6%
2	2.0%	7.7%	15.2	20.6	73.9%
3	3.6%	8.2%	17.4	26.5	65.6%
4	3.9%	5.5%	35.8	38.5	92.8%
5	3.1%	4.1%	47.5	49.6	95.9%

Table 4.7: V_{pp}, I_{pp} and η_{MPPT} for the measurements on array n. 5

At the AC side the inverter performance can be characterized by various kinds of analysis and parameters. In the chapters 5 and 6 are exposed some experimental assessments on real case studies and an approach to the analysis of the power quality fed into the grid. In this section the study is limited to the

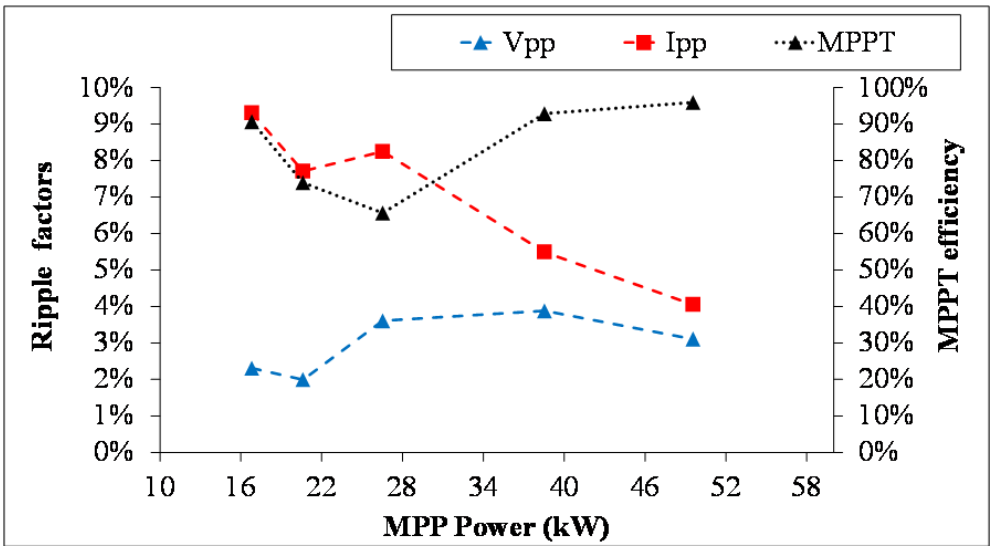

Figure 4.23: DC side inverter efficiency parameters vs. P_{MPP}.

classical DC/AC efficiency, defined as usual:

$$\eta_{DC/AC} = \frac{P_{AC}}{P_{DC}} \tag{4.6}$$

In Fig. 4.24 the results are those expected: the DC/AC efficiency shows values lower than the maximum and European efficiencies declared by the manufacturer, only for low power levels (less than 20% of the nominal power P_n).

4.6 Concluding remarks

From what has been exposed above, it can be safely stated that a BIPV system subject to partial shading phenomenon will expect a great reduction of the power injected to the grid, and, if this issue is constant year-round, also the overall energy produced will be affected. The deformation of the I-V curves can be caused also by the shade over only few cells, even if they are not completely shaded. This deformation, at least in the case studied, can cause a power loss up to 60% of the rated power. Moreover, additional losses are introduced by the MPP tracker of the inverter, since it is not able to follow the absolute maximum on the static

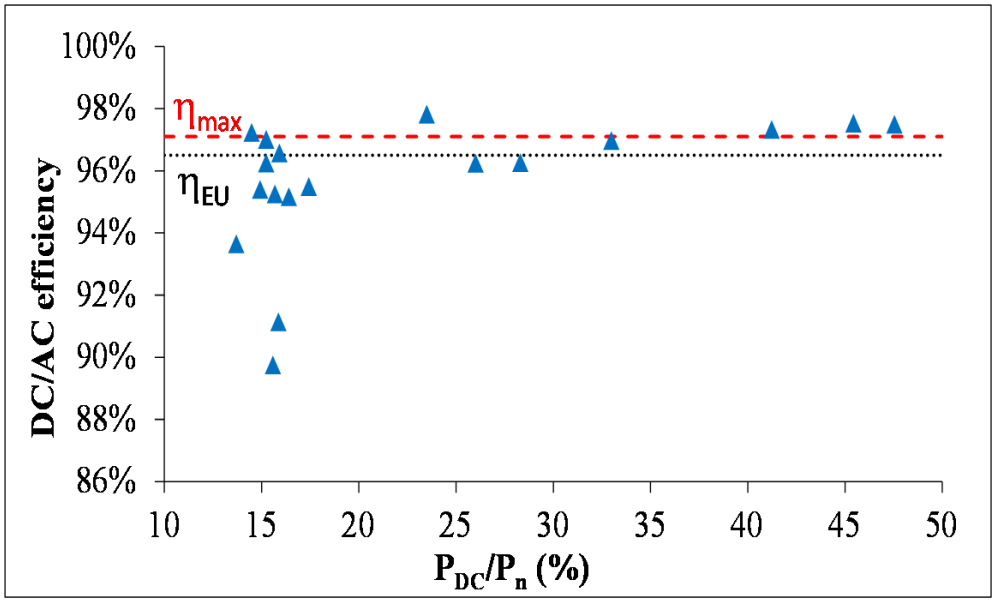

Figure 4.24: DC/AC efficiency of inverter no. 5 vs. P_{DC}/P_n (P_n = 100 kVA).

I-V curve of the PV field. In the analysed case, this loss can reach also the 35%. In comparison the DC/AC efficiency is much less affected by the shading, but nevertheless it can be far from its best values.

This has to be well pondered when designing a BIPV system in an urban environment, since it can result in a strong drawback of the investment. The analysis performed on the case study considered was focused on the I-V mismatch caused by partial shading, since this is the one of the main issues of a BIPV system, but it has a validity in general as a methodology to be applied to other systems with or without other mismatch problems.